DD

SW9435

WIS-94/23/May-PH

The Scintillation of CF_4 and its relevance to detection science

A. Pansky, A. Breskin, A. Buzulutskov[1] , R. Chechik,
V. Elkind and J. Va'vra[2]

Department of Particle Physics
The Weizmann Institute of Science
Rehovot 76100, Israel

ABSTRACT

The scintillation properties of CF_4 are presented in comparison with those of Xe and CH_4. Alpha-particle induced photon emission was measured with vacuum phototubes and with a CsI-based gaseous photomultiplier. The latter method provides an absolute sensitivity of such devices to particle-induced UV-photon background in CF4 and CH4 gaseous Čerenkov radiators.

Integrated CF_4 scintillation yields over the range of 150-220 nm are, on the average, 315±95 to 242±60 photons/MeV, in the respective pressure range of 0.063 to 0.75 atm, compared to CH_4 which emits 0.06±0.1 photons/MeV at 1 atm. The total photon yield, integrated over the full emission spectrum of CF_4 (150-500 nm), is of the order of 1200 photons/MeV·4π.

The primary scintillation photon yield of CF_4 is about 16(±5)% of that of Xe. No proportional secondary scintillation was observed in CF_4. The avalanche-induced photon yield was measured to be of the order of 0.3 photons per electron. The implications of this considerable photon emission, are discussed.

Submitted to Nuclear Instruments and Methods in Physics Research A

---

[1] On leave of absence from IHEP, Protvino, Russia

[2] SLAC, Stanford, CA 94305, USA

1. Introduction

Gas mixtures based on CF_4 have been considered in recent years as counting media in wire chambers[1]. The main advantage is the reduced electron collection time, defined by the high drift velocity. CF_4 has also become an interesting candidate for Čerenkov radiators, due to its high refraction index[2], low chromatic dispersion[3] and high transmission properties in the far UV[4–6] (cutoff around 100 nm). The latter could, in principle, considerably expand the useful wavelength region when detecting the Čerenkov UV-photons with TMAE- or CsI-based gaseous imaging devices. CF_4-based mixtures are also being considered as counting gases in such devices, proposed for fast RICH detectors in future colliders.

On the other hand, CF_4 has been known for some time as a good photon emitter, from the far UV (peak around 160 nm)[6,7] to the visible[8,9]. The emission of CF_4 is mostly attributed to the excited $(CF_3^+)^*$ and $(CF_4^+)^*$ fragments[9]. Except for some recent measurements at atmospheric pressure[6], all other studies refer to very low pressures, in the militorr region. CF_4 was also considered in a gas scintillation chamber for the study of fission fragments[10]. It is a fast scintillator of which the radiative lifetimes, measured at 10 mtorr, are of 2 and 9 ns at 160 nm and 220-300 nm respectively[8]. Being transparent to its own UV-photons, this gas presents serious gain limitations, due to photon feedback, when operating CF_4-filled wire chambers at low gas pressures. We found that the maximal detector gain is lower by several orders of magnitude compared to the operation with hydrocarbons, like isobutane or ethane. Recently, it was also found that a combination of CF_4 and TMAE [Tetrakis (dimethylamine) ethylene] in a wire chamber makes the operation very unstable due to insufficient quenching[11].

We present here the results of some investigations of the photon emission properties of CF_4. The study includes an evaluation of avalanche photon-induced secondary effects and the measurement of the absolute primary and secondary scintillation (de-excitation of gas molecules following collisions with a primary particle or with field-accelerated ionization electrons, respectively) photon yields compared with that of CF_4 and Xe. The implications of the considerable photon emission from CF_4 are discussed.

2. Experimental techniques

The properties such as the primary and secondary scintillation and the avalanche-induced photon emission in CF_4 and their consequences were derived from several experiments involving various techniques described below.

2.1 Photon feedback and avalanche-induced photon yield:

Secondary effects due to photon feedback and avalanche-induced photon yields were measured using an electron counting technique, described in detail in references[12,13]. The detector used, shown in fig. 1, is a double stage parallel plate avalanche chamber coupled to a 33 mm long conversion element, operating at low gas pressure. Both photon feedback and light yield were measured in pure CF_4 and isobutane and in their mixtures. A continuous Hg(Ar) lamp served to measure UV-induced avalanches and their secondary effects; a collimated ^{106}Ru β^- source was used to measure the light yield from avalanches, induced by ionization electrons deposited in the gas.

The avalanche-induced photons were measured using a fast, Philips XP 2020Q, quartz window (cutoff at 165 nm)photomultiplier, coupled to the detector vessel in front of the last electrode mesh. Both optically recorded signals and the charge signals measured at the last multiplication stage, were processed with fast current amplifiers and fed into a PC-driven 1GS/s digitizer for an off-line analysis. For each β-induced ionization electron track (optically or electronically recorded), the number of electron avalanches and their pulse heights were recorded. The normalized light yield, namely the ratio between the photon yield and the number of electrons in the avalanche, was estimated from a summation of the pulse heights of all avalanches in a given event, and taking into account the proper calibration of the amplifiers, the photomultiplier tube (assuming the producer's gain curve) and the relevant solid angle.

2.2 Absolute photon yields:

The absolute, α-induced, photon emission yields (primary scintillation) from CF_4 and CH_4 were measured in a second setup, shown in figure 2. A vessel filled with the emitting gas was coupled to a photosensitive device. A collimated α-source (^{241}Am) was placed in the gas vessel, in front of a solid state detector (SSD). The distance between the source and the SSD defined the energy loss of the alpha particles in the analyzed gas. The solid angle of the detected light was defined by this distance and by the distance of the source to the photosensitive element. Both distances could be adjusted according to the gas and pressure.

The photons were detected by two different photosensors: a vacuum photomultiplier (VPM), Philips XP2020Q, equipped with a quartz window, sensitive in the 165-600 nm range, and a gaseous photomultiplier (GPM), equipped with a CaF_2 window (shown in fig. 2). The latter consists of a two-stage avalanche chamber, operated with CH_4 or C_2H_6, coupled to a CsI photocathode sensitive in the range of 120-220 nm. The photocathode

was produced at our laboratory by vacuum evaporation on a stainless steel substrate.

2.3 Comparison with Xenon:

In a third setup, aiming at the comparison of the primary and secondary scintillation properties of CF_4 with those of Xenon, two types of gas scintillation chambers were used: The first chamber, shown in Fig. 3a, is a scintillation cell irradiated by ^{241}Am α-particles which are stopped at a SSD, in a similar way to that described in 2.2. The primary scintillation in CF_4 and Xenon was measured with a glass-window phototube, Hamamatsu R268, coupled with an optical grease to a quartz (suprasil) window mounted on the gas cell. The inner face of the quartz window was coated, in some experiments, with a p-terphenyl wavelength shifter.

The second chamber (fig. 3b) is a gas scintillation proporational chamber. Alpha particles are stopped in the gas. The ionization electrons drift, under low field, towards the secondary scintillation gap, defined between two parallel grids, 8 mm apart. In this gap a high electric field induces secondary scintillation or gas multiplication. Photons are transmitted via a quartz (Suprasil) window to a Philips phototube XP 2020Q.

High purity gases were used in all cases: CH_4, (99.995%), C_2H_6 (99.99%), Xenon (of 99.995%, further purified on-line in a closed circuit through a BASF Catalyst R3-11 at 230°C) and CF_4 (99.999%, produced by Alphagas Co.). The CF_4 was carefully tested prior to the experiment and was confirmed to have a negligible electron attachment. All measurements were made in a gas flow mode, at pressures varying between a few Torr and one atmosphere, as described below. Data were processed with standard analogue electronics, fast digitizers, and PC-based data acquisition systems.

3. Experimental results

3.1 Photon feedback and avalanche-induced photon yield

3.1.1 Photon feedback

The photon feedback was evaluated by observing secondary electron avalanches, following the UV-induced primary avalanche originating from a photoelectric effect on the first cathode mesh of the detector (see fig. 1). The electric field across the conversion region was reversed, which made this gap non-active in these measurements. A typical pulse trail measured at 9 Torr of CF_4 is shown in figure 4a. Each pulse corresponds to one electron avalanche. The number of pulses in this particular event is 3, corresponding

to a primary avalanche followed by two secondary avalanches. An analysis of the time intervals between consecutive detected electron avalanches, measured for 1000 events at an average gain of $8 \cdot 10^5$, is shown in figure 4b. A well defined characteristic time, of 170 ns, for secondary avalanches to occur is observed. This is due to a photoeffect on the mesh of the preamplification gap. The average number of secondaries in this measurement is 2 per event. Operating the detector with the conversion element active (electron collection mode) and having an Aluminum foil electrode instead of the first mesh (closest to the source, fig. 1) increases the average number of secondary electron avalanches, for an equal gain, by a factor of about 4. This is due to both an efficient photoeffect on the Aluminium foil and an enhanced photoeffect on the meshes by photons reflected from the Aluminum foil. A typical event is shown in figure 5, in which 13 avalanches are observed. A more complex time structure is obtained in this case, due to the contributions of the various electrodes to the photon feedback mechanism.

The exact amount of secondary avalanches depends on the particular geometry of the amplification structures, on the electrode surfaces, on the gas pressure and on the detector gain. The results presented here are only an illustrative example to the intensity of the phenomenon in CF_4 at low pressure.

The photon-feedback effect in CF_4 was observed already at an average gain of $5 \cdot 10^5$, corresponding to the lowest detectable single electron avalanche pulses in our setup. The photon-feedback completely disappeared by adding 20% of isobutane to the CF_4. No secondary effects were observed then, even at detector gains of about $2 \cdot 10^6$. This quenching effect is due to the cutoff of isobutane, at about 170 nm, which makes the detector opaque to the characteristic UV-emission of CF_4 situated around 160 nm.

It should be noted that CH_4 presents similar properties of photon-induced secondary avalanches when operating at low-pressures and high gain[14].

3.1.2 Avalanche-induced photon yield:

The photon yield during amplification, namely the number of photons per avalanche electrons, was measured for CF_4, CF_4/i-C_4H_{10} (80:20) and iC_4H_{10}. The results are summarized in table I. The relatively large uncertainties are due to systematic errors on the photomultiplier gain calibration, and to its unknown absolute quantum efficiency, which was taken as 15% based on the producers' catalogue. From table I we can see that about 60% of the light emitted during amplification in CF_4 is at wavelengths below 300 nm. The addition of 20% of isobutane to CF_4 drastically reduces the light yield, but it is still an order of magnitude larger compared to that measured in pure isobutane.

The large light yield of CF_4 is comparable to that of good known light emitters employed in optical imaging detectors, such as Ar/C_2H_6/TMAE [tetrakis (dimethylamine) ethylene] and other mixtures which include TEA (triethylamine) and TMAE[15–17]. However, the considerable photon feedback in CF_4 may limit its use in optical imaging detectors. The upper limit of the light yield measured here in isobutane is comparable to that measured in ethane[16] under similar conditions.

3.2 Primary scintillation in CF_4 and CH_4

The basic scheme of the experimental setup is shown in fig. 2, for the gaseous photomultiplier readout case. As already mentioned, the solid angle for light emission along the α-track and its collection by the photosensor is a function of the geometrical arrangement of the collimated α-source and the SSD. The effective solid angle was calculated, using a Monte Carlo code, taking into account the reflectivities of the photomultiplier window and the shading effects of the α-source and the SSD housings. The energy loss of the α-particles in the gases investigated was calculated, based on data from Ziegler[18]. The results were confirmed experimentally by observing the residual energy spectra of the α-particles at the SSD. Thus, the energy loss across the α-particle path could be determined with a precision of 10%.

The spectral distribution of photon emission from CF_4, induced by He^+ ions and by electrons, is provided in refs. 7,8; it should be noted that the data are not given in calibrated units. The spectrum has two continua, a principal one peaked around 160 nm and a second extending from 220 to 400 nm, peaked at about 300 nm. The emission spectrum of CH_4 is not known to us.

3.2.1 Measurements using a gaseous photomultiplier:

Measuring the absolute primary scintillation yield with a gaseous photomultiplier (GPM) equipped with a CsI photocathode is of a considerable relevance to the application to Čerenkov Ring Imaging (RICH). Indeed, both CsI (solid) and the TMAE (gas), most considered photosensitive materials in this field, have similar quantum efficiency curve-shapes (within a factor of two), over similar spectral ranges. Therefore, measuring the photon yield with one of these substances provides a direct way to estimate the sensitivity of UV-photon RICH detectors to particle-induced photon background from the Čerenkov radiator.

The method employed here to estimate the UV-photon yield consists of measuring the probability to detect coincidence signals between the gaseous photomultiplier and the

SSD trigger detector.

The GPM was operated under CH_4 or C_2H_6. C_2H_6, though less transparent in the UV, was used in most experiments due to its better operation stability. The cutoff (50% transmission) of C_2H_6 in our present operation conditions (geometry, gas pressure) is estimated to be at 151 nm (see figure (9) in Ref. 19). This is below the lowest known emission wavelength of CF_4[7]. The CsI photocathode was vacuum deposited in on a 60 mm in diameter polished stainless steel disc. Its quantum efficiency was measured with a monochromator system[20,21] before installation in the GPM and after each experiment (to correct for possible deterioration).

Prior to the photon yield measurements the operation conditions of the gaseous photomultiplier were established. Figure 6 shows an efficiency curve indicating an operation plateau. It was obtained by measuring the coincidence rate between the SSD α-particle trigger and the GPM, as function of the voltage at its last multiplication stage.

The absolute photon yield measurements from CF_4 and CH_4 are based on a single photon counting technique. One can get the number of emitted photons using the relation for the probability of "no photon detected", defined as "zero-counting", by:

$$P(0) = e^{-\bar{n}_{det}} = e^{-\bar{n}_\gamma \cdot \eta}$$

where $\bar{n}_{det}$ is the average number of detected photons, $\bar{n}_\gamma$ is the average number of photons emitted by a single α-particle interacting with the gas and η is the photon detection efficiency. The "zero counting" method is described in detail elsewhere[13]. The basic condition for this method is a small percentage of coincidences, of the order of 10-20%.

In this experiment, we measured simultaneously the number of SSD trigger events (S) and the number of SSD-GPM coincidence triggers (C). Random SSD-GPM coincidences (R) were measured by applying a long time delay to the GPM signal (larger than the coincidence circuit gate). The probability of "no photon detected" is related to the experimental rates by $P(0) = 1 - \frac{C-R}{S}$, while the detection efficiency is given explicitly by:

$$\eta = \frac{\Omega}{4\pi} \cdot W_t \cdot M_t \cdot PC_{qe} \cdot Det_{eff}$$

Ω is the solid angle for photon collection by the CsI photocathode, W_t is the CaF_2 window transparency, M_t is the transparency of the detector meshes, PC_{qe} is the CsI photocathode average quantum efficiency, Det_{eff} is the detector efficiency for single photoelectrons. It is known from our previous works that the probability to detect single electrons with low-pressure two-stage avalanche detectors, is close to unity[12,13]. $\bar{n}_\gamma$ is given by $\bar{n}_\gamma = \bar{n}_o \cdot E_\alpha^{gas}$

where E_α^{gas} is the average energy loss of α-particles in the gas (in MeV), and $\bar{n}_o$ is the average number of photons produced per 1 MeV.

The results of the primary scintillation $\bar{n}_o$ in CF_4 for 4 different geometrical configurations (solid-angle and source-SSD distance) are plotted in fig. 7 as function of the gas pressure. The primary scintillation value measured for CH_4 is 0.06 (+14%-18%) photons/MeV·4π. The systematic errors of this procedure are the following: solid-angle ($\pm$10%), photocathode QE ($\pm$10%), detector efficiency (-10%). The systematic error on the energy loss in the gas is increasing with decreasing pressure, which enlarges the total error at the lower pressure range. The detector efficiency was assumed to be 100% (see fig. 6).

Despite the large uncertainty, a slight systematic decrease in the primary scintillation yield $\bar{n}_o$ with pressure is apparent. It could be due to a wavelength shifting of the emitted photons (to a region with lower CsI quantum efficiency values) due to collisions of excited CF_4 molecules. Another possibility could be some absorption of photons by oxygen and water impurities in CF_4. However this possibility cannot explain the experimental results since the self absorption of the particular CF_4 gas was measured, with a different vessel, using a monochromator system. It was found to be inferior to 5% at 1 atm, over a gas length of 300 mm.

Our measurements indicate that the absolute α-induced photon emission yield of CF_4, in the sensitivity region of CsI, varies between 315 $\pm$ 90 photons/MeV·4π at 0.0625 atm to 242 $\pm$ 60 photons/MeV·4π at 0.75 atm.

3.2.2 Measurements using the vacuum photomultiplier:

Photons induced by a known amount of energy deposited in CF_4 by the α-particles were detected also by a vacuum photomultiplier (VPM, see Sec. 2.2). The measurements were taken at different gas pressures, and with different filters of which the indicated cut-off values were measured by us: an Aclar foil (210 nm), a 280 nm filter and a Plexiglass plate (360 nm). The average number of photoelectrons measured by the VPM are summarized in table II, for a CF_4 pressure of 0.5 atm.

In principle, using the quantum efficiency curve of the VPM provided by the manufacturer, one can defold these data to obtain the number of photons emitted from the gas. This is given in Table III. The large uncertainties in the photoelectron numbers (Table II) lead to very large uncertainties in the photon yield.

One can notice that the number of UV-photons measured by the two methods in

the spectral range of 150-220 nm is different. However, taking into account the higher confidence level of the CsI-based GPM results, we may conclude that the valid number for the photon yield in this range should be of the order of 300 photons/MeV·4π as discussed in 3.2.1.

This photon yield and the ones measured with the VPM at the higher spectral range, with a better confidence level, will be used in the following for light yield comparison with Xe, using a p-terphenyl wavelength shifter.

3.3 Comparison with Xenon

The primary scintillation and the secondary scintillation, i.e. the photon emission under electric field, were measured in the same setup for Xenon and CF_4. Fig. 8 shows pulse-height spectra of primary scintillation induced by ^{241}Am α-particles in both gases, measured with a glass-window phototube, with and without a p-terphenyl wavelength shifter. The data were recorded for events triggered by the SSD. For an equal source-to-SSD distance, the gas pressure was adjusted so as to have in both gases the same energy deposit. As is evident from Fig. 8 a,b, the phototube response to CF_4 scintillation is about 27% of that of Xe.

We also measured the primary scintillation in CF_4 and Xe with a quartz-windowed phototube (XP 2020Q) coupled by a UV- transparent optical compound to the quartz window of the chamber. The gas was excited with α-particles. The ratio of CF_4-to-Xe primary scintillation response (using this particular phototube), shown at the origin of the graphs in fig. 8, is of the order of 60%. The ratio between the photon yields in the two gases, based on the p-terphenyl data, will be calculated and discussed in section 4.

The light yield as function of the electric field is shown in fig. 9. While the well-known secondary scintillation in Xe, (ending at about 6 kV/cm·atm), clearly appears and obeys the linear field dependence, no proportional secondary scintillation is observed in CF_4. The light yield steeply rises in a proportional avalanche multiplication mode. This behaviour supports a model that positive ions CF_3^+ or CF_4^+ may be the emitting species. It means that the emission under electric field can occur only after the gas ionization commencement, i.e., during the gas multiplication mode.

4. Discussion and summary

We discuss first the results of the three experiments on the measurement of the CF_4 scintillation yield: two experiments on the primary photon yield, using the gaseous and

vacuum photomultipliers (GPM and VPM), and one on the photon yield relative to Xe, using a vacuum photomultiplier having a glass window coated or uncoated with a p-terphenyl wavelength shifter.

The first two experiments complement each other. Indeed the photon yield in the region of the first emission continuum, around 160 nm, was measured with a good accuracy using the CsI-based GPM, while using the VPM, the region of the second emission continuum, centered around 300 nm, was measured with sufficient accuracy as discussed in 3.2.2. Combining these data we roughly estimate that about 300 photons/MeV·4π are emitted in the first continuum (below 200 nm, GPM results) and about 800 photons/MeV·4π in the second continuum (VPM, see last three columns in table II). Thus the total number of photons emitted by CF_4 over the whole spectral range is estimated to be of the order of 1100 $\pm$ 300 photons/MeV·4π.

In spite the fact that the efficiency of p-terphenyl is constant below 340 nm [22], one cannot extract the relative photon yield from the ratio of the CF_4-to-Xe photomultiplier response (see 3.3), without the exact knowledge of the relative CF_4 emission spectrum. Indeed, as one can see from table III, a significant amount of photons are emitted above 340 nm, i.e., in the region where p-terphenyl does not function as a wavelength shifter. Therefore, only a rough estimation can be done using the data of Fig. 8a-c and taking into account the available data on CF_4 emission distributions. In our setup the p-terphenyl layer was at a distance of 5 mm from the photomultiplier photocathode. This leads to a geometrical reduction factor of 0.28, to be included in the calculations of the light yield for this case. The difference between the data of Fig. 8b and 8c is indeed due to this geometrical factor. Taking into consideration also the quantum response of p-terphenyl[23] and its spectral response[22], the difference in the emission solid angles between the data in figures 8b and 8c, the optical parameters and the quantum efficiency of the phototube, we estimate the total photon yield of CF_4 to be about 16($\pm$ 5)% of that of Xe. It should be noted that a recent work reports on a 36% increase in the primary scintillation of Xe with an admixture of 5% CF_4[24].

The absolute value of the induced photon yield in Xe is not given in the literature. We therefore calculated this yield taking as a reference the absolute α-induced yield in NaI(Tl)[25], the relative scintillation efficiency of Xe reduced to that of CsI (Tl) and the one of CsI (Tl) reduced to that of NaI (Tl)[26,27]. We obtain a yield of 7200 photons/MeV·4π. Based on this number we estimate the total photon yield in CF_4 to be of about 1200 photons/MeV·4π. About 75% of these photons are emitted above 220 nm. This is in agreement with the numbers discussed above in 3.2. We may therefore conclude that the

data on CF_4 primary scintillation photon yield, obtained by different techniques and in different experimental setups are coherent, within the large uncertainties of the rather different experimental conditions.

The considerable particle-induced UV-emission prevents its use in Čerenkov radiators coupled to UV imaging detectors operating with TMAE or TEA photosensitive vapors or with CsI photocathodes. The large avalanche-induced emission, when used without admixtures, inhibits its use as a high gain counting gas. On the other hand, one could suggest the use of CF_4-based gas mixtures in combination with optical readout systems[16,17]. These could be beneficial in the fields of particle tracking, photon imaging and electron counting.

The fact revealed in the present work, that CF_4 is a very good scintillator, indicates the direction in which one could search for new, high-Z, gas or liquid scintillators. Indeed, in refs. 28,29 a light emission from some other freons, such as CF_3Cl or CF_3Br, has been observed at low pressure. They were reported to have quite similar emission continua and photon yields to that of CF_4. We may speculate that CF_3I can scintillate as well. If their scintillation properties are conserved at higher pressure or even in the liquid phase, the materials of the type of CF_nX_m (X=Cl, Br, I, etc...) could compete with liquid Xe or Kr as low cost, high-Z, scintillation detection media.

This work was supported by the Foundation Mordoh Mijan de Salonique, by the Basic Research Foundation of the Israel Academy of Sciences and Humanities, and by the United States-Israel Binational Science Foundation (BSF). A. Buzulutskov is grateful to the Feinberg Graduate School for his support.

gas	average gain	normalized light yield photons/electrons	remarks
CF_4	1.5E6	0.30	165-600 nm
CF_4	1.5E6	0.10	Mylar window, cutoff at 300 nm
CF_4/i-C_4H_{10}(80:20)	4.4E6	0.022	170-600 nm
i-C_4H_{10}	5E6	$\leq$ 5E-3	170-600 nm

Table I The ratio of the number of emitted photons (over 4π) to electrons in an avalanche, measured in a double-stage parallel plate detector with different gas mixtures at 9 Torr. The systematic errors in the gain calibrations are of 20% and in the normalized light yield are of 50%.

Spectral range [nm]	165-600	210-600	280-600	360-600
photoelectrons/MeV·4π	280±39	202±33	160±27	56± 25

Table II: The average number of α-induced photoelectrons, detected by the VPM using different filters, in 0.5 atm CF_4.

Spectral range [nm]	165-210	210-280	280-360	360-600
photons/MeV·4π	1110±730	210±220	420±150	220±100

Table III:The average number of α-induced photons detected by the VPM in different spectral bands. The data are derived from the values of table II and the supplied quantum efficiency of the VPM.

References

1. See for example J. Va'vra, Nucl. Instrum. and Meth. **A323** (1992) 34 and references therein.
2. R. Abjean, A. Bideau-Mehu and Y. Guern, Nucl. Instrum. and Meth. **A292** (1990) 593.
3. T. Ypsilantis and J. Seiguinot, Nucl. Instrum. and Meth. **A343** (1994) 30.
4. Y. Giomataris, G. Charpak, V. Peskov and F. Sauli, Nucl. Instrum. and Meth. **A323** (1992) 431.
5. M. Chen et al. Preprint CERN-PPE/93-191.
6. J. Friese et al., the HADES project, private communication.
7. J.F.M. Aarts, Chem. Phys. Lett. **114** (1985) 114 and references therein.
8. J.E. Hesser and K. Dressler, J. Chem. Phys. **47** (1967) 3443.
9. U. Muller, T. Bubel, G. Schulz, A. Sevilla, J. Dike and K. Becker, Z. Phys. **D24** (1992) 131 and references therein.
10. J. Handschun, R.A. Walters, R.T. Schneider and E.E. Carrol, IEEE Trans. Nucl. Sci. **NS-20** (1973) 633.
11. J. Va'vra, J. Kadyk, J. Wise, and P. Coyle, "Study of Photosensitive mixtures of TMAE and Helium, hydrocarbon and CF_4-based carrier gases", to be published in Nucl. Instrum. and Meth.
12. A. Pansky, A. Breskin, R. Chechik, and G. Malamud, Nucl. Instrum. and Meth. **A330** (1993) 150.
13. G. Malamud, A. Breskin, R. Chechik, and A. Pansky, J. Appl. Phys. **74** (1993) 3645.
14. A. Breskin, G. Charpak, S. Majewski, Nucl. Instrum. and Meth. **220** (1984) 349.
15. D. Sauvage, A. Breskin, and R. Chechik, Nucl. Instrum. and Meth. **A275** (1989) 351.
16. A. Breskin, R. Chechik and D. Sauvage, Nucl. Instrum. and Meth. **A286** (1990) 251 and references therein.
17. G. Charpak et al., IEEE Trans. Nucl. Sci. **NS-35** (1988) 483, and references

therein.

18. J.F. Ziegler, The stopping and ranges of ions in matter, Vol. 4, Pergamon press, 1977.

19. A. Breskin, Fast low-pressure UV-photon detectors for Čerenkov Ring Imaging, in Proc. of the Int. Symp. of Particle Identification at High Luminosity Hadron Colliders (ed. T.J. Gourlay and J.G. Morfin) FNAL (1989) p.255.

20. H. Brauning, A. Breskin, R. Chechik, P. Miné and D. Vartsky, Nucl. Instrum. and Meth. **A327** (1993) 369.

21. A. Breskin, R. Chechik, D. Vartsky, G. Malamud and P. Mine, Nucl. Instrum. and Meth. **A343** (1994) 159 and references therein.

22. I.B. Berlman, Handbook of fluorescence spectra of aromatic molecules, Academic Press NY (1971) p.220.

23. V. Kumar and A.K. Datta, Appl. Optics **18** (1979) 1414.

24. C. Broggini, Nucl. Instrum. and Meth. **A345** (1994) 503.

25. J.B. Birks, The theory and practice of Scintillation Counting, Pergamon Press, Oxford (1964).

26. A.J.P.L. Policarpo, Space Sci. Instr. **3** (1977) 77.

27. G. Bertollini, A.M. Del Turco and G. Restli, Nucl. Instrum. and Meth. **7** (1960) 350.

28. H.A. Van Sprang, H.H. Brongersma and F.J. De Heer, Chem. Phys. **35** (1978) 51.

29. L.C. Lee, J.C. Han, C. Ye and M. Suto, J. Chem. Phys. **92** (1990) 133.

Figure captions

Fig. 1. The experimental setup employed for measuring photon-induced secondary avalanches and the photon yield in the avalanche process. Ionization or photon-induced electrons are multiplied in two stages. Pulses induced by the primary and secondary avalanches are recorded electrically or optically (see text).

Fig. 2. The experimental setup employed for measuring the primary scintillation induced by α-particles in CF_4 and CH_4. Photons emitted from the gas are detected through a CaF_2 window by a gaseous photomultiplier (GPM) combining a CsI photocathode and a low-pressure two-stage electron multiplier (see text).

Fig. 3. The experimental arrangements employed for comparing scintillation properties of CF_4 and Xe. Primary scintillation is induced in the gas (a) by α-particles and is detected with a vacuum photomultiplier. Secondary scintillation is produced (b) by accelerating the ionization electrons in a parallel gap and the light is detected with a vacuum photomultiplier.

Fig. 4. An example of a UV-induced avalanche pulse trail in 10 Torr CF_4(a) showing the original avalanche pulse followed by two secondary avalanche pulses. It was measured in the setup shown in fig. 1, with a reversed field in the conversion volume. The sharp distribution of the time intervals between successive avalanche-induced pulses (b) indicates that the secondary effects originate from photoelectrons created at a defined surface.

Fig. 5. An example of a UV-induced pulse trail in 10 Torr CF_4, measured in the setup shown in fig. 1, with the conversion volume active. The considerable yield of avalanche pulses following the primary avalanche, indicates the intensity of the secondary effect.

Fig. 6. An efficiency graph of the ethane-filled gaseous photomultiplier (GPM), indicating a plateau at the MWPC anode voltages exceeding 780V.

Fig. 7. The absolute α-particle induced UV-photon yield measured in the setup shown in fig. 2, as function of the pressure in CF_4. The measurements were done at different solid angles, indicated in the figure.

Fig. 8. The response of a vacuum photomultiplier with a glass window, coated with p-terphenyl (a,b) and uncoated (c), to the α-particle induced primary scintillation in Xe and CF_4. The deposited energy in the gas, monitored by a SSD, is the same in each case.

Fig. 9. The relative photon yield from Xe and CF_4 under electric field. While Xe clearly exhibits secondary proportional scintillation, in CF_4 the steep rise following primary scintillation is due to proportional multiplication and no secondary scintillation is observed.

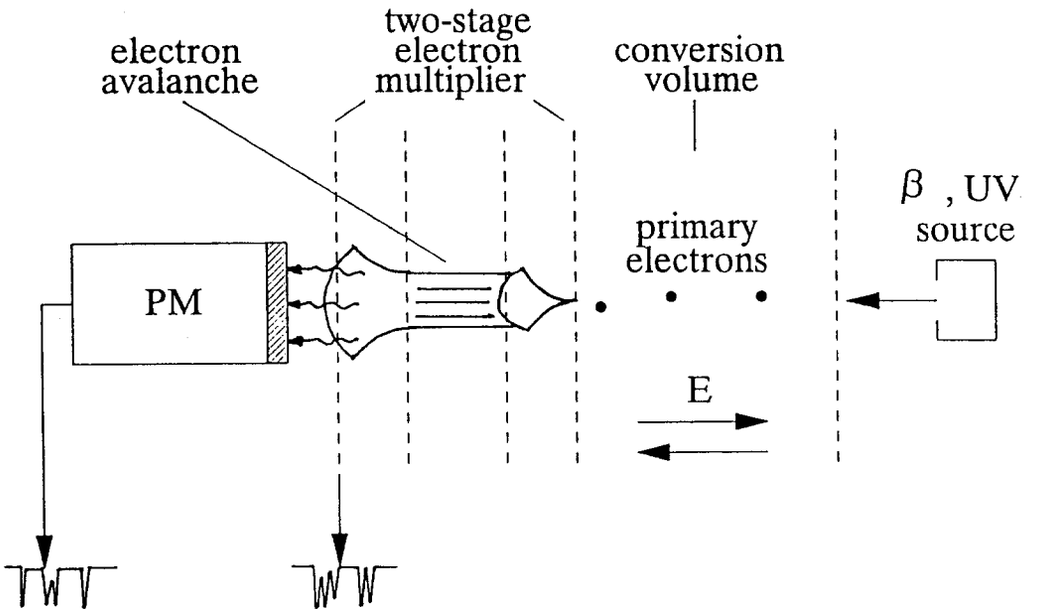
electron
avalanche
two-stage
electron
multiplier
conversion
volume
β , UV
source
primary
electrons
PM
E

Fig.1

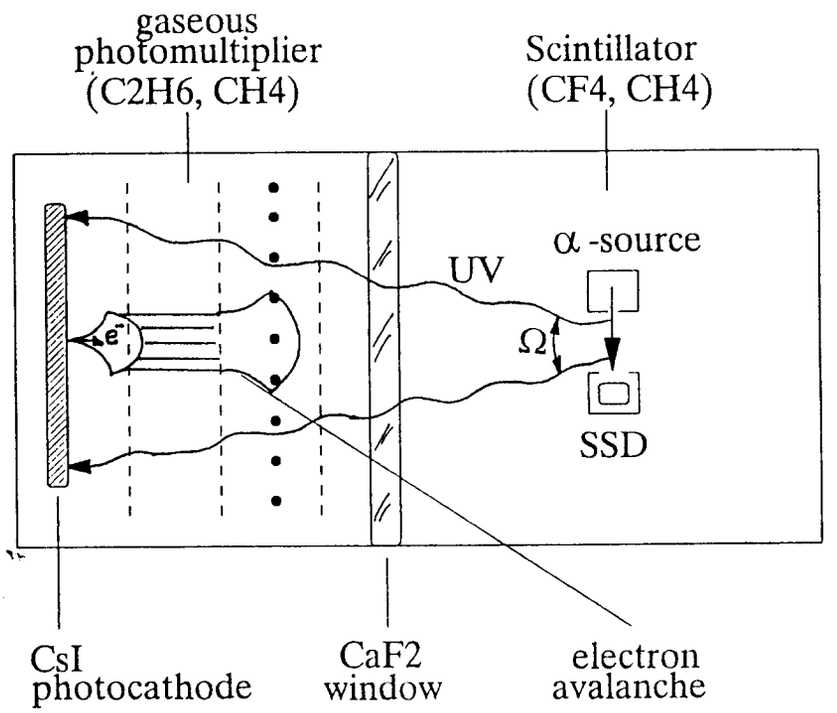
gaseous
photomultiplier
(C2H6, CH4)
Scintillator
(CF4, CH4)
α -source
UV
Ω
SSD
CsI
photocathode
CaF2
window
electron
avalanche

Fig.2

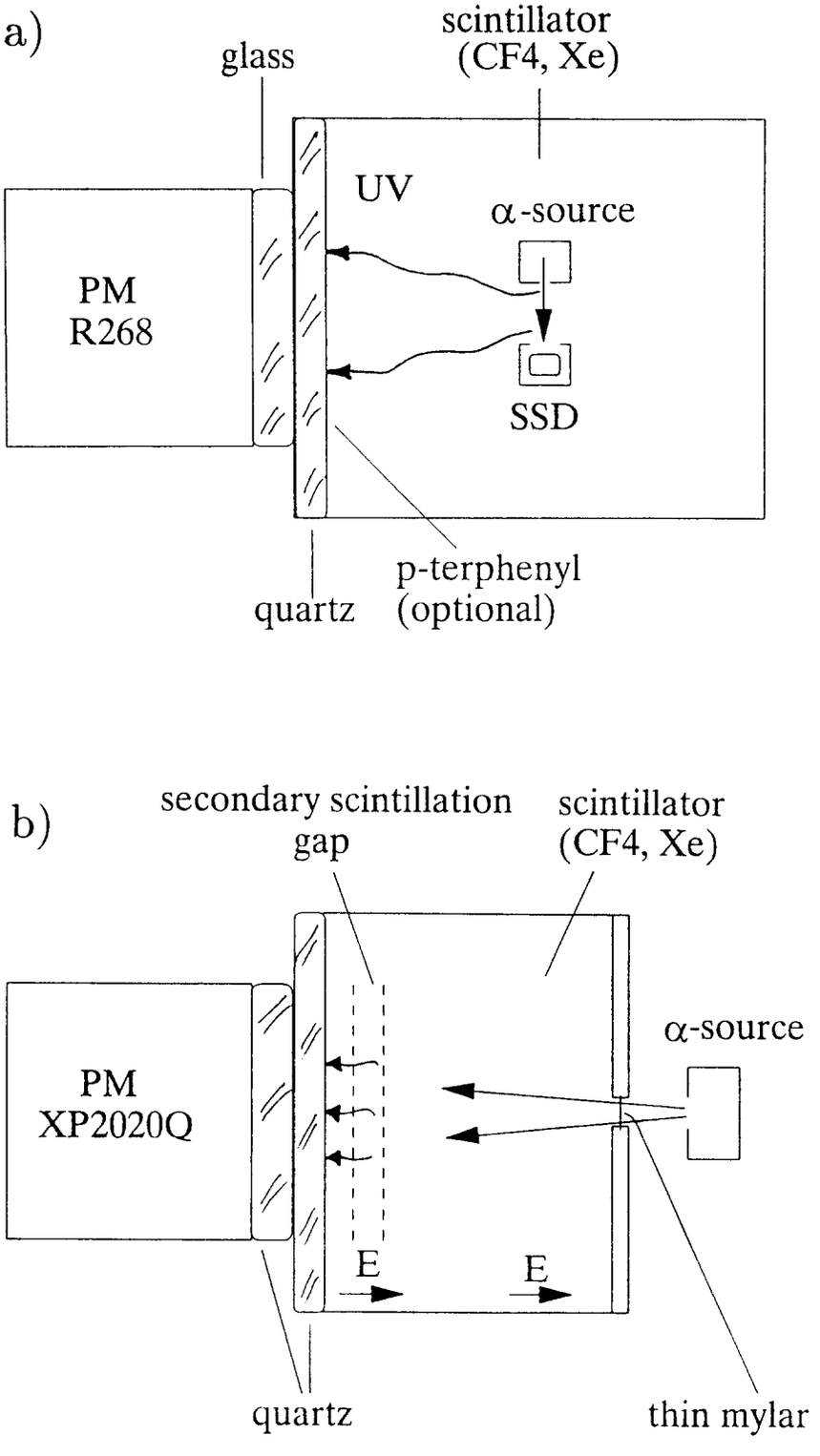
a)
glass
scintillator
(CF4, Xe)
UV
α-source
PM
R268
SSD
p-terphenyl
(optional)
quartz
b)
secondary scintillation
gap
scintillator
(CF4, Xe)
α-source
PM
XP2020Q
E
E
quartz
thin mylar

Fig.3

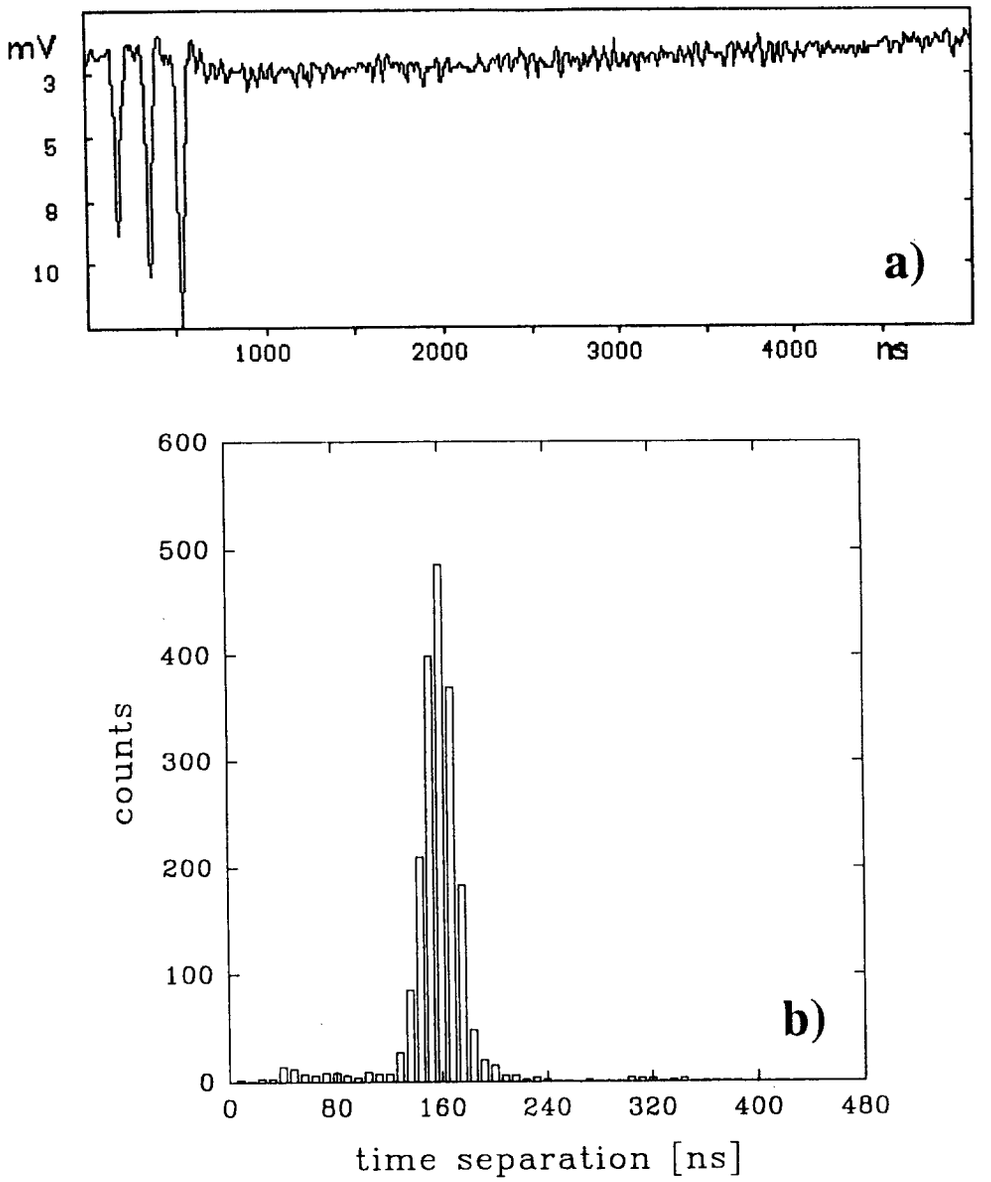
mV
3
5
8
10
a)
1000
2000
3000
4000
ns
600
500
400
300
200
100
0
counts
b)
0
80
160
240
320
400
480
time separation [ns]

Fig.4

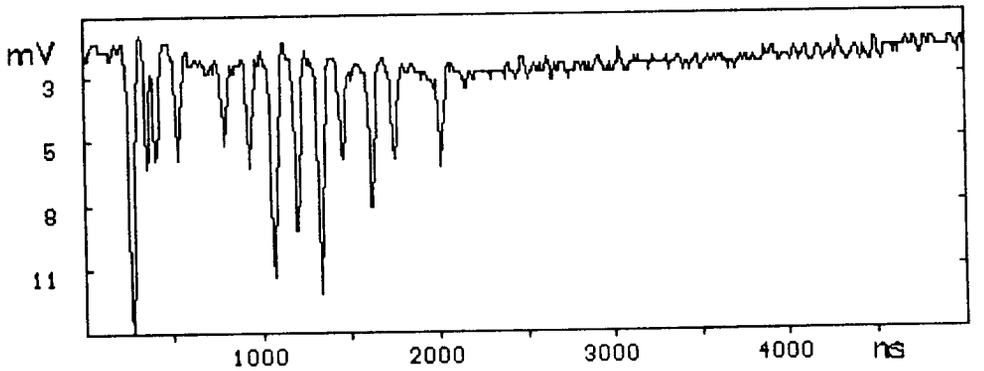
mV
3
5
8
11
1000
2000
3000
4000
ns

Fig.5

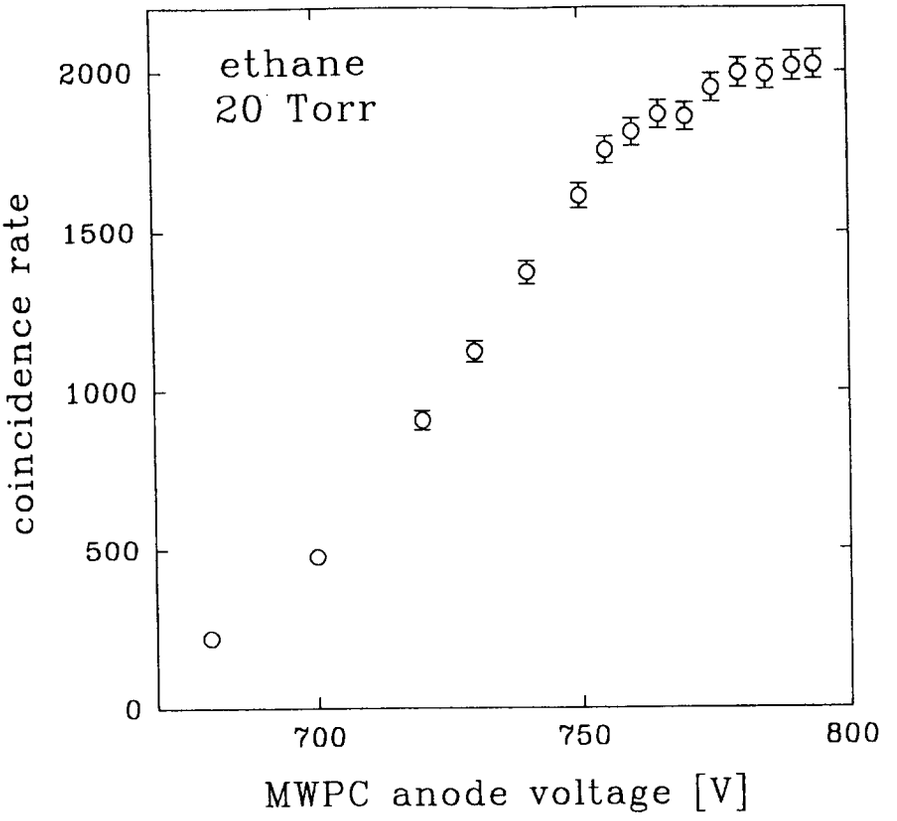
ethane
20 Torr
coincidence rate
2000
1500
1000
500
0
700
750
800
MWPC anode voltage [V]

Fig.6

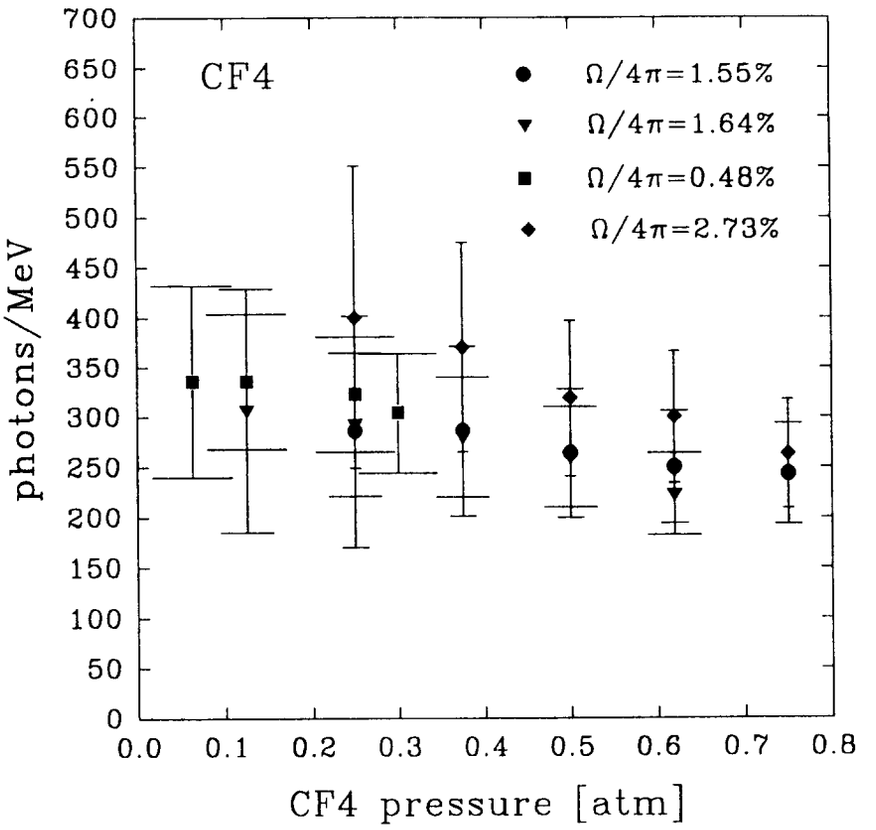
CF4
Ω/4π=1.55%
Ω/4π=1.64%
Ω/4π=0.48%
Ω/4π=2.73%
photons/MeV
700
650
600
550
500
450
400
350
300
250
200
150
100
50
0
0.0
0.1
0.2
0.3
0.4
0.5
0.6
0.7
0.8
CF4 pressure [atm]

Fig.7

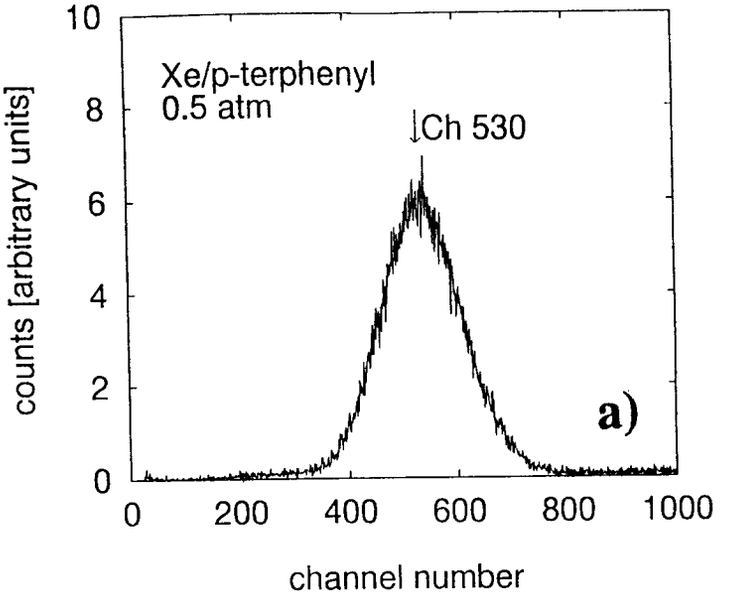
Xe/p-terphenyl
0.5 atm
Ch 530
a)
counts [arbitrary units]
channel number
0
2
4
6
8
10
0
200
400
600
800
1000

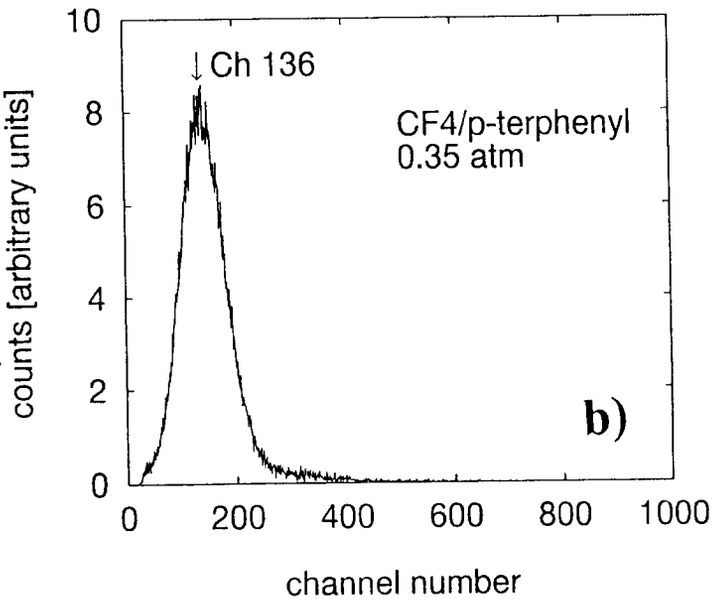
Ch 136
CF4/p-terphenyl
0.35 atm
b)
counts [arbitrary units]
channel number
0
2
4
6
8
10
0
200
400
600
800
1000

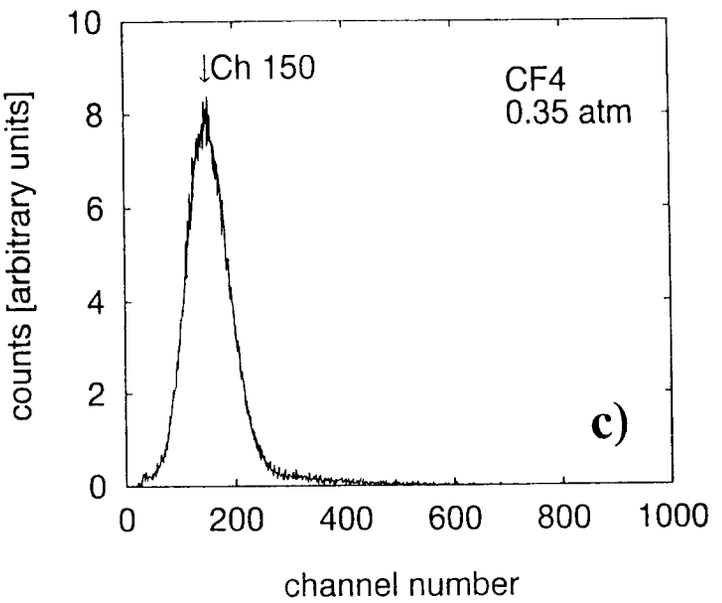
Ch 150
CF4
0.35 atm
c)
counts [arbitrary units]
channel number
0
2
4
6
8
10
0
200
400
600
800
1000

Fig.8

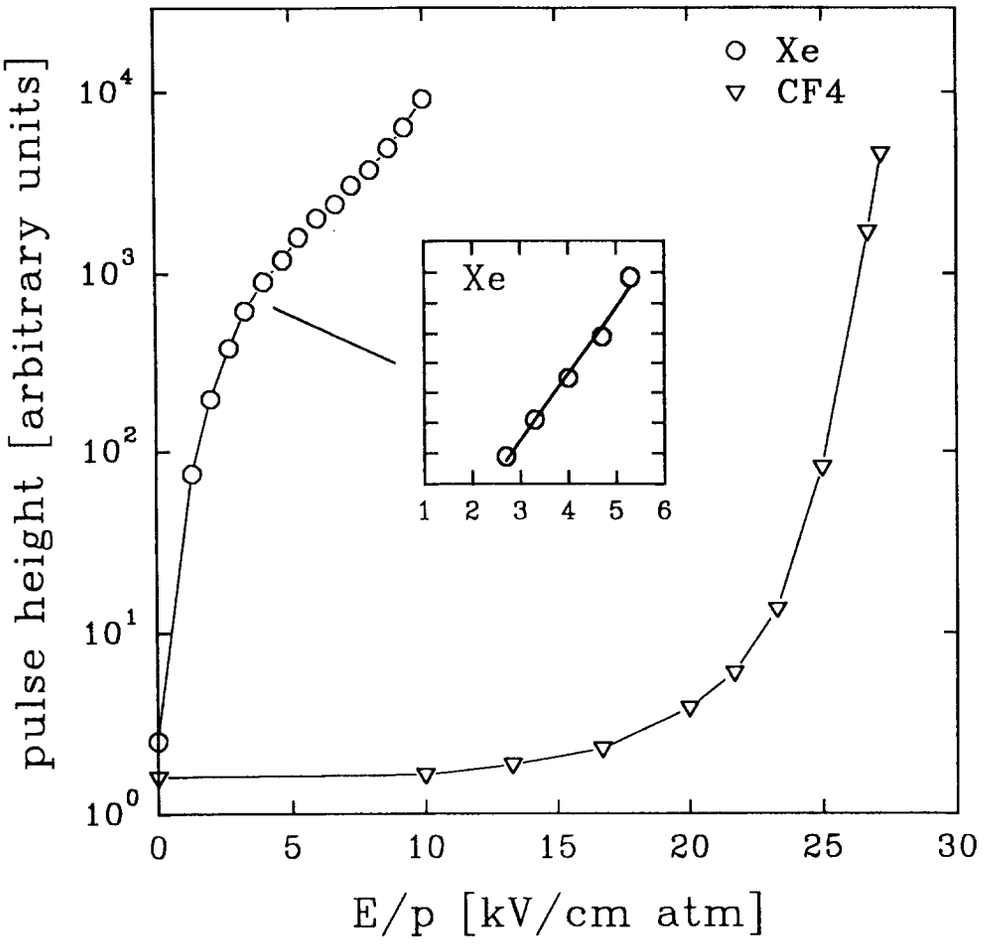
pulse height [arbitrary units]
10^4
10^3
10^2
10^1
10^0
0
5
10
15
20
25
30
E/p [kV/cm atm]
Xe
CF4
Xe
1
2
3
4
5
6

Fig.9